Pacific Northwest
NATIONAL LABORATORY

PNNL-35420

Blockchain for Fault-Tolerant Grid Operations Version 2.0

December 2023

Fernando Bereta dos Reis
Mark Borkum
Monish Mukherjee
Hayden M Reeve
David J Sebastian Cardenas

U.S. DEPARTMENT OF ENERGY

Prepared for the U.S. Department of Energy
Under contract DE-AC05-76RL01830

DISCLAIMER

PACIFIC NORTHWEST NATIONAL LABORATORY
operated by
BATTELLE
for the
UNITED STATES DEPARTMENT OF ENERGY
under Contract DE-AC05-76RL01830

Printed in the United States of America

Available to DOE and DOE contractors from the
Office of Scientific and Technical Information,
P.O. Box 62, Oak Ridge, TN 37831-0062;
ph: (865) 576-8401
fax: (865) 576-5728
email: reports@adonis.osti.gov

Available to the public from the National Technical Information Service
5301 Shawnee Rd., Alexandria, VA 22312
ph: (800) 553-NTIS (6847)
email: orders@ntis.gov <https://www.ntis.gov/about>
Online ordering: http://www.ntis.gov

PNNL-35420

Blockchain for Fault-Tolerant Grid Operations Version 2.0

December 2023

Fernando Bereta dos Reis Mark Borkum
Monish Mukherjee Hayden M Reeve
David J Sebastian Cardenas

Prepared for
the U.S. Department of Energy
Under Contract DE-AC05-76RL01830

Pacific Northwest National Laboratory
Richland, Washington 99354

Abstract

This report explores the potential of distributed ledger technology (DLT) as a transformative tool to enhance fault-tolerant operations in electrical distribution systems. This study focuses on three critical use cases that leverage DLT's core attributes, including an immutable decentralized ledger, distributed consensus mechanisms, and state replication capabilities.

A central aspect of this research is the utilization of a consensus-driven ledger, providing actors within the system, such as distributed energy resources, with access to a reliable data repository. This empowers these actors to collaborate effectively and make informed decisions, all securely recorded on the blockchain. The first use case concentrates on data configuration, utilizing mathematical criteria—particularly, the chi-squared test for gross error detection—to identify trustworthy sensors for advanced decision-making. Building upon this foundation of trust, the second use case, topology identification, accurately determines circuit breaker states, unveiling the distribution network's topology. Ultimately, the third use case leverages this trust to execute switching actions, reconfiguring feeders and restoring power to disconnected customers after fault events.

The concept of trust serves as a cornerstone in this approach, marking a departure from traditional fault location, isolation, and service restoration (FLISR) methods. Additionally, the DLT-based architecture introduces decentralization, empowering disconnected areas to make autonomous decisions, even when communication with a central control center is disrupted. The primary contributions of this report are twofold: (1) a novel approach for evaluating distribution system voltage areas while preserving data ownership and (2) the implementation of interactions between distribution network areas using the actor model. Unlike the previous sequential approach in the previous report named "Blockchain for Fault-Tolerant Grid Operations" number PNNL-33981, for evaluating the area connection voltages, which required a radial network topology, this study's area model reduction method enables a more versatile approach. The area model reduction method addresses issues of prolonged data waiting times and multiple points of failure within the previous approach. Notably, the presented evaluation for the reduced network model area connection reveals a significant increase in the differences in voltage magnitudes.

Simulation and evaluation of area agents across four distinct cases elucidate the area-level interaction behavior during a fault event. Simulations demonstrate that the proposed distributed FLISR (DFLISR) approach can successfully restore service to an affected area. Varying message delays and message loss probabilities in each simulation case underscore their impacts on restoration times, ranging from 3 min and 32 s to 6 min and 19 s. In contrast, power is not restored in an area in one of our simulation cases.

Acronyms and Abbreviations

BDI	belief, desire, and intention
CAP	consistency, availability, and partition tolerance
DFLISR	distributed fault location, isolation, and service restoration
DLT	distributed ledger technology
DSO	distribution system operator
FLISR	fault location, isolation, and service restoration
PNNL	Pacific Northwest National Laboratory
SCADA	supervisory control and data acquisition
SE	state estimation
UCR	utility control resource
UML	Unified Modeling Language

Acknowledgments

This project was supported by the Department of Energy (DOE), Office of Electricity's Advanced Grid Research and Development Program. The authors would like to thank Chris Irwin of DOE for their support of this study.

Contents

Figures

Tables

1.0 Introduction

Power distribution systems serve as the backbone of electric power delivery to millions of customers, covering vast geographical expanses. Typically, these distribution systems are organized in a radial configuration, where each segment of the system plays a pivotal role in ensuring uninterrupted customer connectivity. Distribution power systems exhibit a higher susceptibility to faults compared to transmission and generation systems. These faults can originate from various natural factors, including, but not limited to, severe weather conditions, natural disasters, vegetation encroachment, equipment malfunctions, and even deliberate malicious attacks (Bompard et al., 2013). It is crucial to emphasize that every segment of the distribution network is susceptible to failure, and the likelihood of failures occurring increases as the network's scale increases. Given the radial nature of distribution systems, the failure of a single component can lead to the disconnection of downstream customers and equipment. In practice, approximately 80% of all customer disruptions can be attributed to faults or outages within distribution networks (Gonen, 2015). To gain a comprehensive understanding of the causes of these faults, Department of Energy (DOE) (2014) conducted a meticulous analysis utilizing feeder-level data obtained from nearly 300 documented outage incidents across five utility companies in the United States.

One strategy for mitigating customer disruptions in the event of a persistent fault involves the utilization of a fault location, isolation, and service restoration (FLISR) algorithm. This algorithm facilitates the reconfiguration of a distribution system's topology through a centralized controller and is used for permanent faults[1]. An autonomous and distributed solution known as distributed FLISR (DFLISR) holds the potential to enhance the resilience of the grid (Bhattarai et al., 2021). In a related context, a multiagent DFLISR approach is elucidated in (Tsai and Pan, 2011), where the distribution system is partitioned into distinct zones and switch regions. This approach leverages agents guided by the principles of belief, desire, and intention (BDI) to formulate effective strategies for various operational scenarios. In contrast, Leniston et al. (2022) introduce a centralized FLISR approach tailored for distribution networks enriched with a substantial quantity of distributed resources. It is worth noting that neither Tsai and Pan (2011) nor Leniston et al. (2022) delve into the intricate challenges posed by sensor errors and inaccurate system knowledge. While FLISR mechanisms can autonomously initiate restorative actions in cases of degraded operational modes, their automated recovery processes expose them to potential vulnerabilities from malicious actors. These actors possess the capability to manipulate sensor data, thereby deceiving FLISR systems regarding the true operational state. This manipulation could lead to misoperations such as unwarranted disconnection of customers under normal operating conditions.

In recent years, the adoption of blockchain and distributed ledger technology (DLT) has witnessed a notable surge within the realm of electric power engineering. An extensive survey, which exclusively delves into the utilization of DLT for transactive energy, is presented in (Siano et al., 2019). This survey rigorously assesses both the advantages and challenges associated with employing DLT in peer-to-peer energy trading scenarios. The study's findings highlight DLT's potential to enhance energy transactions by rendering them more efficient, secure, and transparent. Furthermore, it demonstrates the capability of DLT to reduce transaction costs and enable the development of innovative business models. In (Abdella et al., 2021), the authors propose a detailed architectural framework tailored for peer-to-peer energy trading, seamlessly integrating DLT. This framework considers the establishment of virtual power plants and microgrids, fostering an online marketplace wherein prosumers and consumers can directly

[1] Permanent faults, which cannot be resolved by simply tripping and reclosing, present a particular challenge. In the absence of a recloser, all faults are classified as permanent.

exchange energy resources. The authors meticulously evaluate the performance of this architecture, assessing key aspects such as scalability, security, and efficiency. Hayes et al. (2020) introduce a co-simulation environment that serves as a comprehensive platform for investigating peer-to-peer energy trading dynamics. Their research explores the repercussions of transactive energy within the constraints of electricity distribution networks. It is important to note that Nour et al. (2022) offer an exhaustive review, encompassing aspects such as energy trading, metering and billing, the enhancement of power system cybersecurity, and the operation and management of power systems. While their discourse on challenges for large-scale adoption extends beyond market operations, it provides valuable insights into the broader implications of DLT. In (Di Silvestre et al., 2019), they harness blockchain technology to deliver ancillary services within a microgrid context, diligently considering network limitations. The constraints inherent in energy management communities are also addressed in (Van Cutsem et al., 2020). To tackle cybersecurity concerns in smart grids, Zhuang et al. (2021) present an extensive survey, specifically focusing on the blockchain's role. Furthermore, Sharma et al. (2018) conduct a survey concerning the cybersecurity of the Internet of Things within a blockchain-based distributed cloud architecture.

This report also delves into the various blockchain-based solutions proposed to counteract cybersecurity challenges in smart grids, encompassing secure data sharing, communication, and control. In (Liang et al., 2019), a protective framework based on DLT is proposed to safeguard power systems against cyberattacks, thereby ensuring the integrity of ledger-protected data used in smart grid applications such as load forecasting, local redistribution, and demand response. The authors explore potential pathways, including the integration of DLT into distribution networks, with the aim of stabilizing voltage profiles. In a practical demonstration of DLT's capabilities, an approach handling large-scale data and sensors at a remarkable sampling rate of up to 10 kHz is elaborated in (Hahn et al., 2022). This report underscores the feasibility of the proposed DLT methodology, with a specific focus on substations and control centers, enabling attestation and detection of suspicious changes on a significant scale.

In summary, it has become evident that the blockchain and DLT offer multifaceted advantages in the domain of electric power engineering:

1. enhanced trust in data capture processes
2. improved topology identification and augmentation of the system's visibility
3. preparing for innovative DFLISR solutions.

Furthermore, the use of a unified ledger, localized within a service region, facilitates traceability, even across various operational boundaries such as multiple distribution system operators (DSOs).

1.1 Study Objective

The main goal of this study is to demonstrate the role that DLT can have in improving the fault tolerance of power distribution systems. Three specific fault-tolerance use cases were developed, as listed in our previous report (Bhattarai et al., 2021), and expanded into detailed Unified Modeling Language (UML) diagrams in our follow-on report (dos Reis et al., 2023). The approach separates the distribution network into switch-delimited distribution network areas. The main contributions of this study are:

- A new approach for evaluating a distribution system voltage area that preserves data ownership is presented
- An actor model is used to implement the interactions between distribution network areas.

The previously proposed approach for evaluating the area connection voltage required a sequential approach in which the network must be radial, and the vast majority of distribution systems are operated radially. This requirement limits the approach's applicability to all distribution system networks. The other two limitations of the sequential approach are:

1. the increased time that given areas must wait for data to be provided by the previous area in the connection path to perform its portion of the analysis
2. the creation of multiple points of failure, given that any failure to provide analyses on the path stops the analysis from being concluded.

Developing interactions between distributed elements as actors is a key focus of this study. The primary capability of the developed actor model environment is to evaluate how the distributed approach would behave.

1.2 Report Structure

The remainder of this report is structured as follows. Section 2.0 presents an overview of the operation of a distribution system and DLT applications. It provides the fundamentals for developing fault-tolerant grid operations by leveraging DLT. Section 3.0 presents the engineering requirements for each of the proposed use cases, focusing on how DLT can functionally help a distribution system maintain operations under fault conditions. Section 4.0 describes the developed actor model environment. Section 5.0 presents a comparison of the approaches for evaluating the area connection and the behavior of DLT for DFLISR use cases for multiple temporal and message-passing characteristics. Finally, Section 6.0 presents the conclusions and plans for future work.

2.0 Technical Background

2.1 Distribution Systems

Power systems confront a myriad of vulnerabilities arising from various sources, encompassing natural factors such as adverse weather conditions, environmental catastrophes, the proliferation of vegetation, equipment malfunctions, and deliberate attacks (Bompard et al., 2013). Distribution systems play a pivotal role in catering to a diverse spectrum of customers, spanning residential, commercial, and industrial sectors. The infrastructure components are scattered across extensive geographical expanses. Failures can manifest at any point within the distribution network, and a network with a larger scale has greater susceptibility to potential breakdowns. Given the prevalent radial configuration of distribution systems, the malfunction of any individual component can lead to the disconnection of downstream customers and equipment. It is noteworthy that an astonishing 80% of all disruptions in customer service can be attributed to faults and outages occurring within distribution networks (Gonen, 2015). Figure 1 illustrates a comprehensive breakdown of the diverse factors contributing to faults in distribution systems. This breakdown is derived from feeder-level data extracted from nearly 300 documented outage incidents across five prominent utility companies in the United States.

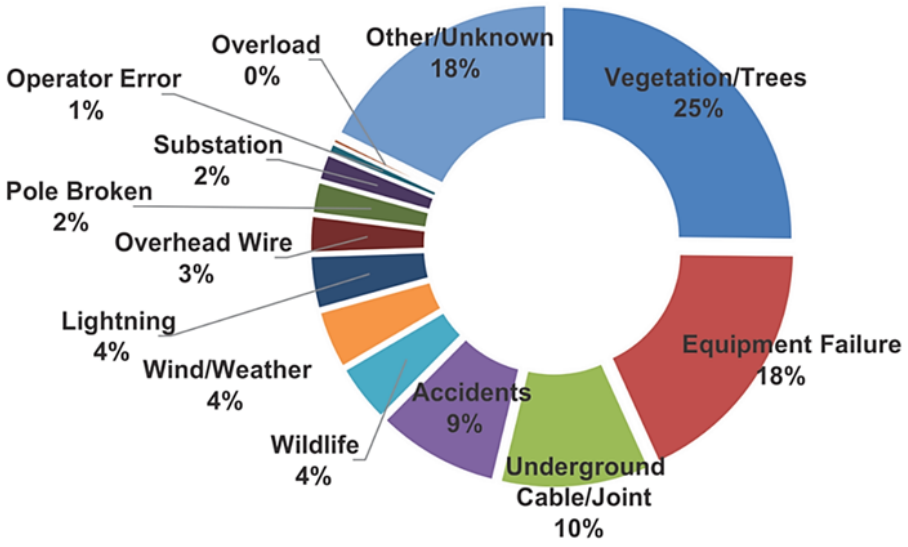

Figure 1: Causes of distribution system faults. Image from (Department of Energy (DOE), 2014).

In instances of permanent failures within distribution networks, maintenance teams are tasked with identifying faults and implementing appropriate remedies. The time required for restoration hinges on several factors, including the availability of replacement components, workforce scheduling, the geographical location of the faulty equipment, and the availability of necessary tools and resources. Permanent faults in distribution networks can result in the disconnection of customers until alternative power solutions are devised. To mitigate disruptions and minimize their economic impact, alternative energy pathways are designed based on fault assumptions, ultimately leading to the reconfiguration of the distribution network's topology. The FLISR process relies on a coordinated automation approach, involving various components such as feeder switches, reclosers, communication networks, supervisory control and data acquisition (SCADA) systems, and historical data. Figure 2 illustrates the key stages of the

FLISR process, which encompass fault localization, segment isolation, and re-energization. A prevalent strategy for enhancing the effectiveness of FLISR is the centralization of data. This approach provides the FLISR strategy with real-time situational awareness regarding the current state of the distribution network.

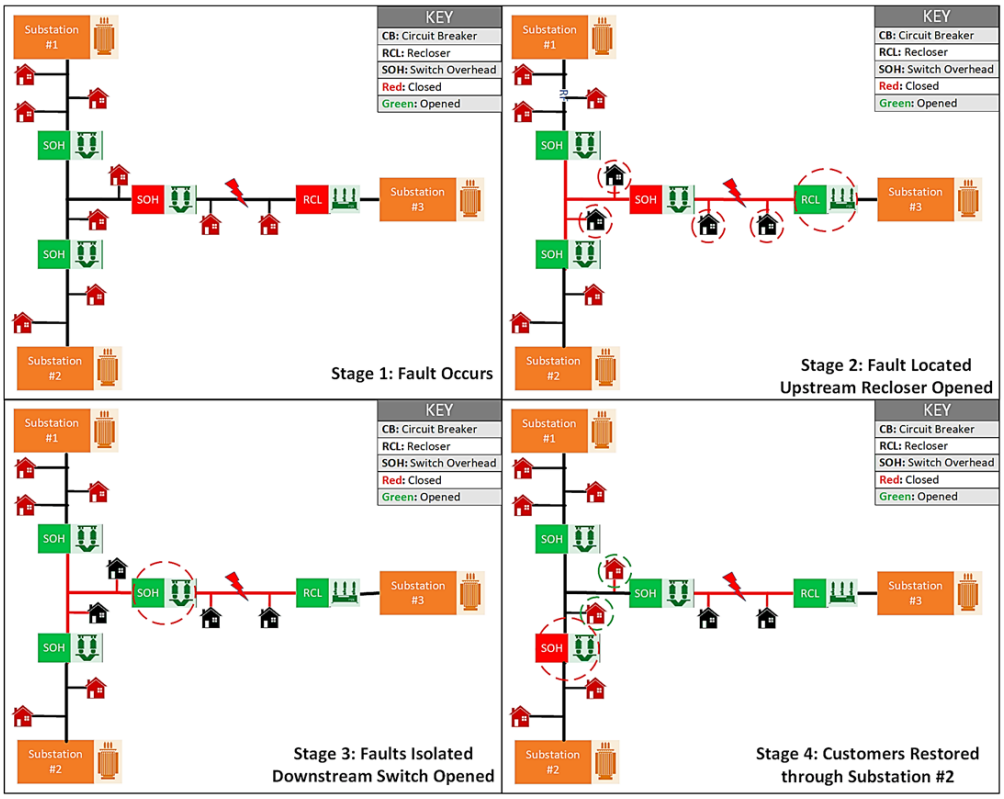

Figure 2: Typical utility fault-handling process utilizing FLISR. Image source: (Department of Energy (DOE), 2014).

FLISR systems play a pivotal role in minimizing the areas affected by permanent failures within distribution networks by altering the network topology. Ideally, these systems aim to isolate only the specific areas affected by the failure, thereby ensuring uninterrupted power supply to the rest of the network. However, this automated recovery mechanism also makes FLISR systems attractive targets for malicious actors. For instance, adept manipulation of sensor data can deceive an FLISR system regarding its current operational status, potentially leading to misoperations such as unwarranted customer disconnections during routine network operations. In alignment with critical engineering imperatives, FLISR systems are obligated to maintain fail-safe operational conditions to effectively counteract both natural and malevolence-induced events. An additional vulnerability inherent in traditional FLISR systems is their centralized architecture, where applications are concentrated at a central control center. This configuration introduces a single point of failure while underutilizing the available resources within the field and across adjacent DSOs. Leveraging its distinctive architectural characteristics, blockchain technology holds the promise of enhancing confidence in the authenticity of data generated within the distribution network. This enhancement enables applications like FLISR to make more informed decisions while concurrently reducing the risk of misoperations.

2.2 Key Elements of Distributed Ledger Technology

DLT encompasses a diverse set of technical components that collaboratively establish a platform capable of hosting a globally distributed state. These constituent elements can be succinctly described as follows:

1. Immutable Ledger: At the core of DLT lies an interconnected series of data blocks, secured using cryptographic hashes, forming an immutable ledger. Attempting to modify past records necessitates altering these hashes, a process that readily exposes any tampering attempts. This ledger maintains an exhaustive historical record and is redundantly stored across multiple participants within the network.

2. Consensus Mechanisms: In a DLT system, participants must reach consensus on actions leading to block creation and their sequential arrangement. While consensus mechanisms are typically tailored to specific DLT implementations, the choice of mechanism can be customized to meet specific user requirements. The dichotomy between permission-based and fully decentralized solutions presents distinct advantages and drawbacks. Notably, permissioned DLT implementations have gained favor in power systems due to their ability to link digital identities with physical service addresses and enhance computational efficiency.

3. Credential Management: Ensuring security enhancements within DLT implementations requires robust credential management. This encompasses the digital identification of the requesting entity affixed to a new block and the tracking of the endorsement process, which identifies the peers that sanctioned the request. These features, dependent on the DLT framework, encompass aspects such as entity registration, renewal, and revocation (both through self-management and centralized entities); access control via digital identities; and the facilitation of low-level application programming interface access (e.g., proposing new smart contracts).

4. Distributed System Architecture: Central to the foundation of DLTs are well-established designs that govern the architecture of distributed systems. This framework ensures seamless communication among network participants and the eventual establishment of consensus, all within the context of the consistency, availability, and partition tolerance (CAP) theorem. According to this theorem, a distributed system can simultaneously maintain any two out of three essential characteristics: (a) consistency, where systems unanimously agree on stored data; (b) availability, ensuring every request receives an appropriate response; and (c) partition tolerance, allowing system operation despite disruptions among participating agents. Incorporating diverse methodologies for voting and data ordering to maintain data consistency significantly contributes to the overall robustness of the system.

By encapsulating these facets, DLT forms a multifaceted ecosystem that delivers benefits across various domains, with particular relevance in the field of power systems.

3.0 Methodology

Drawing upon the insights gained from the comprehensive literature review, we have identified three distinct use-case scenarios that leverage the fundamental capabilities of DLT to enhance the robustness of fault-tolerant grid operations. These use cases have been meticulously crafted to ensure the secure implementation of a distributed FLISR system. As previously emphasized, FLISR algorithms are vulnerable to potential malicious interventions, where threat actors may attempt to compromise the system's integrity by tampering with critical components, including the system model, sensor data, and the statuses of switching devices. Such actions can jeopardize the utility resources involved in the DFLISR process. By harnessing DLT's intrinsic ability to maintain an immutable ledger, we inherently bolster the security of the system model. Given that sensor data and the statuses of switching devices are dynamic and require continuous assessment, two of these use cases work in concert to ensure ongoing evaluation of the system's state, thereby instilling confidence in the data utilized. In scenarios where utility resources may be compromised, DLT's distributed consensus mechanisms assume a pivotal role in preserving the integrity of the system. The three elucidated use-case scenarios for enhancing fault-tolerant grid operations encompass the following: (1) DLT-driven configuration of grid data, (2) utilization of DLT for topology discernment, and (3) incorporation of DLT for the distributed FLISR process. These use cases form interconnected and cohesive modules, collectively contributing to a comprehensive solution. The integration of these modules is visually represented in Figure 3.

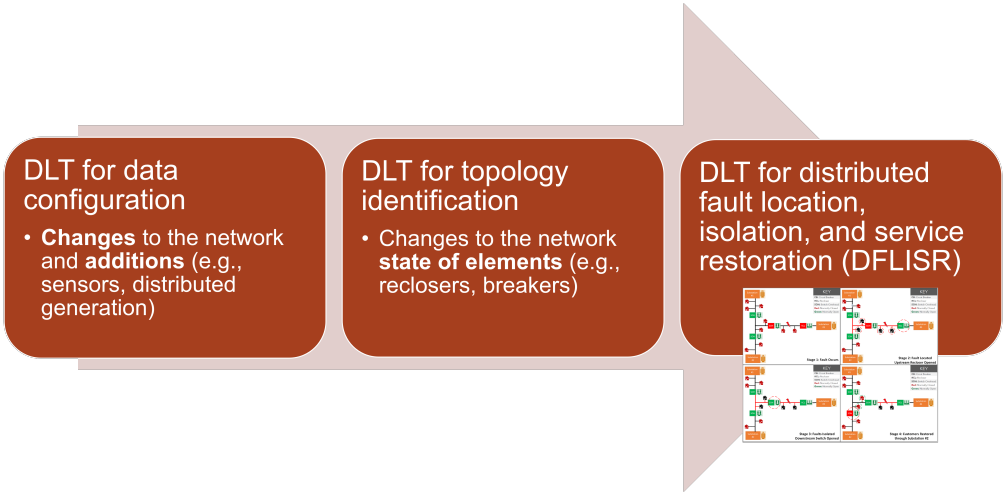

Figure 3: Dependency map for DLT-based use cases, demonstrating each module's ability to support higher-order functions such as DFLISR. Image source: (dos Reis et al., 2023).

The utilization of DLT in grid-data configuration serves as a fundamental "trust anchor" that consolidates sensor measurements, thereby establishing the most precise representation of the current system state. This trusted dataset forms the bedrock for informed decision-making and reinforces fault-tolerant grid applications, particularly DFLISR. This report exclusively delves into these specific use cases while acknowledging that there exist broader potential applications for situational awareness beyond its scope.

The implementation of these use cases substantially enhances the decision-making capabilities of the DFLISR system. They are endowed with a robust system perspective, validated by multiple entities through consensus mechanisms. This layer of trust complements the conventional state estimation (SE) algorithms commonly found in SCADA systems, thereby

introducing an additional level of error detection capabilities. Cyber-physical attacks that target SE algorithms may involve the manipulation of state-based measurements, compromising time-series-based measurement data, and manipulation of the network model (Bretas et al., 2017). In particular, manipulating the network model poses a significant challenge, as SE algorithms assume network stability, with changes attributed solely to physical alterations. The immutable ledger provides perpetual verification of the network model's lineage. By monitoring switching device operations, discrepancies in the topology can be promptly identified, triggering manual examination when deemed necessary. Once the integrity of both the topology and sensor measurements is affirmed, judicious control measures can be initiated, including the coordination of distributed resources.

3.1 Distributed Ledger Technology Capabilities for Distributed Fault-Tolerant Architectures

To realize the scenarios depicted in Figure 3, the establishment of an effective distributed architecture that adheres to business constraints becomes imperative. In the initial stages of design, a solution architect may presume uniform ledger access for all utility agents, including sensors, actuators, and services. While this approach facilitates comprehensive system verification, it introduces certain limitations. Chiefly, the thorough examination of every measurement and network detail necessitates significant computational resources, resulting in substantial communication overheads and heightened security vulnerabilities. Furthermore, consensus networks involving numerous participants often suffer from inefficiency, failing to enhance fault tolerance. Lastly, relying exclusively on a single ledger complicates data segregation among competing entities, necessitating client-side encryption for confidentiality, thereby compromising the advantages of public auditability.

This report presents a solution to overcome these challenges by advocating a segmented-ledger strategy built upon a multilevel ledger framework. This approach involves the partitioning of data into discrete "areas," with a top-tier ledger dedicated to preserving interarea information. The proposed methodology is succinctly illustrated in Figure 4. The local area ledger in the diagram encapsulates local measurements and a simplified network model. This enables field devices, characterized by limited computational capabilities, to perform comprehensive area assessments. However, the state of each area remains contingent upon neighboring area states, necessitating an understanding of boundary conditions, including power transmission into other areas through tie points.

The segmented-ledger approach empowers each area to engage with adjacent areas, irrespective of ownership, as long as a physical, direct, or indirect connection exists. The system ledger predominantly archives static information, encompassing area network model details, conceivable direct/indirect area connections, and potential physical interarea associations in its communication roster for each area. Network data stored within the system ledger are expected to exhibit relative stability, with periodic updates reflecting physical alterations. In contrast, the area ledger anticipates continuous updates, documenting the current area status, sensor performance, and potential reconfigurations.

Of significant note, utility-controlled assets bear the responsibility of assessing and coordinating topology shifts based on local network area conditions. Additionally, they manage external reconfiguration requests. Figure 4 provides a graphical representation of the computational resources within each local area, including utility-controlled entities, a dedicated area manager, and dedicated sensor additions entrusted with overseeing potential sensor augmentations.

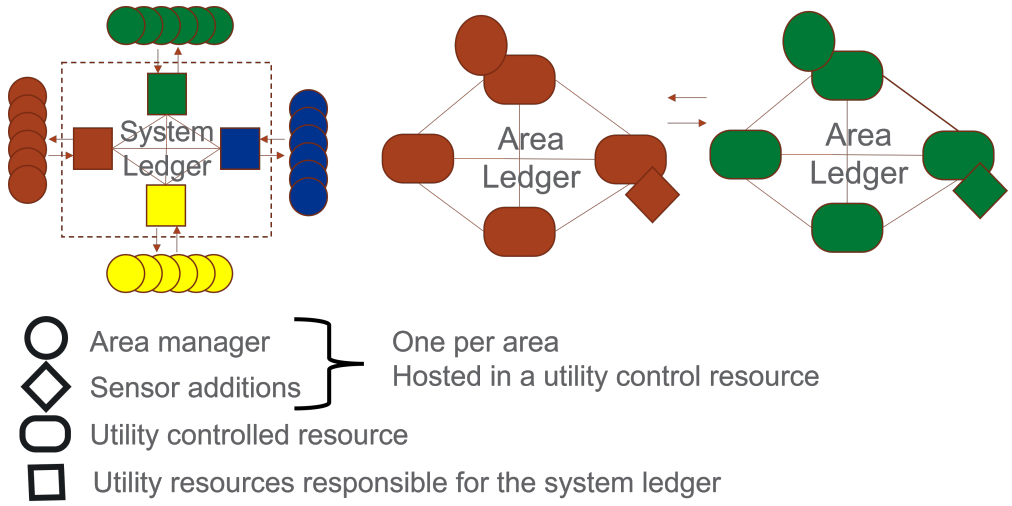

Figure 4: DLT architecture for fault-tolerant grid operation. The focus of this report is on the area ledger. Image source: (dos Reis et al., 2023).

3.1.1 Requirements for Data Exchange

The utilization scenarios depicted in Figure 4 are rooted in a distributed, fault-tolerant architectural framework. Presently, our primary focus is showcasing the functionalities, particularly those related to the local area ledger, from an area-centric standpoint. The journey of the area ledger commences by validating the availability of an up-to-date network model (Y_{bus}). It then proceeds to compile nodal information, the reduced network model (Y_{bus_r}) for other areas, the area communication list, potential area connections, and the power flows originating from tie points. The roster of neighboring areas is derived from tie-point data, pinpointing areas that could be influenced by or influence local decision-making processes.

Within this framework, the local area manager, often implemented via a smart contract, perpetually monitors the ledger's state and reports faults to initiate an FLISR event when necessary. Following an FLISR event, the area manager takes on the responsibility of assembling feasible reconnection strategies. These strategies aim to restore services within the region or facilitate the reconnection of an external area, thereby incorporating the local area into a broader reconnection path.

Shifting from a conventional point-to-point communication architecture to a shared ledger infrastructure introduces fault tolerance characteristics inherent to distributed networks while concurrently mitigating the risks associated with message-level manipulations. Such manipulations could entail intentionally altered measurements or the introduction of malicious control signals. For the acquisition of grid measurements, a smart contract can administer the sensor addition process. This approach effectively eliminates single points of failure and empowers sensors to employ a consensus mechanism to validate the legitimacy of each collected measurement.

Upon registration, actors receive credentials that enable authentication against peers and ensure comprehensive tracking of all actor activities within a region, facilitated by the area manager. These credentials are intricately linked to the actor's physical grid interface, typically the point of interconnection. Consequently, actors are exclusively permitted to engage in subregions where their observations and actions hold relevance and validity.

3.1.2 UML Summary Descriptions from the Previous Effort

In our prior report (dos Reis et al., 2023), we provided an extensive discussion and detailed UML description. This UML modeling focuses on the utility control resource (UCR) and its role in executing essential tasks for DLT use cases in fault-tolerant grid operations within distribution networks. Figure 5 illustrates the overall behavior of these use cases during both normal and FLISR operations. Normal operation encompasses the DLT use cases for data configuration and DLT for topology identification, as depicted in Figure 3. The DLT for DFLISR operation is detailed under the FLISR operation category. Our approach for sequential area connection, presented in Section 3.2, was previously presented in our aforementioned report (dos Reis et al., 2023). Additionally, we introduce a novel approach for evaluating the network model area connections in Section 3.2.2. This new methodology, similar to the sequential approach, leverages SE. For a detailed exposition of the SE utilized, please refer to our prior report (dos Reis et al., 2023).

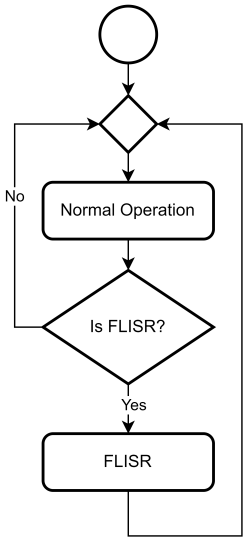

Figure 5: Simplified view of the transition function. The “normal” operation state refers to the ability to supply electrical power to its customers, and the “FLISR” operational state is where at least a portion of the system is outside the normal operation state. Image source: (dos Reis et al., 2023).

3.2 Computing the Voltages of the Areas to be Reconnected

To facilitate the reconnection of an area, it is essential to determine its nonculpability for the fault and establish the feasibility of establishing a connection. Merely considering the potential for reconnection is insufficient to initiate the necessary modifications. To undertake the alterations effectively, the proposed system must offer a viable solution. This report subsequently delineates two subsections: the first outlines the conventional approach for assessing a feasible solution, assuming a radial topology, while the second introduces a novel, nonsequential approach that is independent of the radial topology assumption.

3.2.1 Sequential Area Connection Evaluation

The methodology relies on treating downstream areas as electrical loads and subsequently computes the terminal voltage employing the SE algorithm. This approach is highly effective for radial distribution systems, which constitute the prevalent topology among distribution network feeders. However, certain distribution systems utilize a ring topology, necessitating a more robust voltage drop calculation technique. Nevertheless, the proposed voltage drop calculation method offers the advantage of simplicity in terms of input data requirements. Each area merely needs knowledge of its own demand profile, specified at the node level, and the net demand of downstream areas that require power supply. This approach ensures the preservation of interarea consumer privacy since it involves sharing only an aggregated demand value and the computed tie-point voltage magnitude with adjacent areas. Additionally, by assuming that the voltage magnitude at the initial tie point linking the first feeder area to the substation remains approximately constant at 1.0 pu, a viable solution can be derived without factoring in the upstream transmission system.

To illustrate this approach, consider a radial feeder subdivided into three areas, with interconnections between each area through tie points, as depicted in Figure 6.

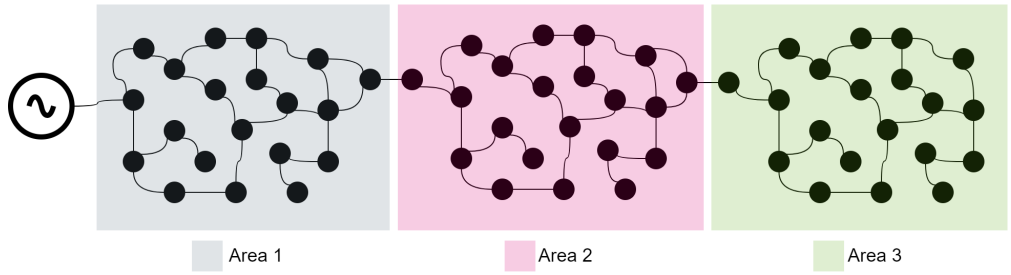

Figure 6: Three areas connected by tie points to illustrate the voltage drop calculation procedure for radial systems. Black dots represent nodes.

The procedure for evaluating the feasibility of a reconnection path and determining the voltage for Area 3 is as follows:

1. Area 1 possesses information about the source bus voltage, per-node load distribution within Area 1, and the anticipated load contributions from Area 2 and Area 3 as observed from the tie point. With these data, it calculates the voltage magnitudes at all nodes, including the tie points, within Area 1.

2. If it meets the area-specific criteria, Area 1 shares the tie point's voltage magnitude with Area 2.

3. Building upon the voltage magnitude provided by Area 1, Area 2 employs SE to compute the voltage magnitude for all its nodes. This computation considers the load at each node in Area 2 and the expected load from Area 3, which is treated as a load connected to the tie point.

4. Should it satisfy the area-specific criteria, Area 2 transmits the tie point's voltage magnitude to Area 3.

5. Area 3 utilizes SE, taking into account the voltage data supplied by Area 2 and a comprehensive breakdown of the loads within Area 3, to estimate the bus voltage magnitudes within

its domain. If the voltage profile adheres to the specified criteria, the reconnection path is deemed feasible and can be documented as a valid option within the ledger.

The described approach involves multiple stages for evaluating the feasibility of reconnection when multiple areas are part of the reconnection path to Area 3. The number of steps required corresponds to the number of areas involved in the reconnection path, resulting in $O(n)$ operations. These processes are executed independently by actors representing different areas. Initialization and updates to the system information are sourced from the system ledger. The pertinent information encompasses potential area connections, substation connections, the net demand by area, and the tie-point associations among areas. This empowers the area seeking reconnection to generate potential reconnection routes, allocating a location for accommodating the net demand. Consequently, this approach results in an FLISR methodology that operates without the need for communication with the system-level ledger during an event.

3.2.2 Reducing the Network Model Area Connection Evaluation

The sequential approach necessitates that the network follows a radial topology. The vast majority of distribution systems indeed operate with a radial configuration. However, this requirement confines the applicability of the approach, limiting its use to radial distribution system networks. Furthermore, there are two additional constraints associated with the sequential approach. First, it prolongs the time required for areas along the connection path to receive the data from preceding areas, delaying their own analysis. Second, it introduces multiple points of failure, as any interruption in the transmission of analysis along the path halts the entire analysis process. The extended time not only affects the duration of customer disconnection but can also render the reconnection infeasible, as there is a limited window available for making changes to prevent energizing areas undergoing maintenance.

To address the limitations of the sequential approach, reduced network models are employed, allowing a single area to conduct the analysis. However, this approach necessitates that the area in question possesses information from the other areas. To maintain network information from these other areas while not providing the actual network model, a network model reduction technique is implemented. Nevertheless, network reduction poses several challenges, as reducing the network dimensions can affect accuracy. It is worth noting that the primary focus of this study is not on network model reduction, but the strategy employed here is consistent with the approach documented in PowerWorld software training (PowerWorld Corporation, 2008). Figure 7 provides an illustration of the network model reduction process.

The network model's admittance matrix denoted as Y in (1) is divided into buses belonging to the study system (indexed as S) and external buses (indexed as E). Simultaneously, we represent the vectors for voltage (V) and current (I) pertaining to the network buses. When we apply (1) with the objective of eliminating the external buses, we obtain (2). In this equation, $Y_{S,S}$ represents the admittance matrix for the study system. The term $-Y_{S,E}Y_{E,E}^{-1}Y_{E,S}$ gives rise to the new equivalent lines connecting the boundary buses and the shunt elements at these boundary buses, while $Y_{S,E}Y_{E,E}^{-1}I_E$ represents the equivalent currents at the boundary buses.

$$\begin{bmatrix} I_S \\ I_E \end{bmatrix} = \begin{bmatrix} Y_{S,S} & Y_{S,E} \\ Y_{E,S} & Y_{E,E} \end{bmatrix} \begin{bmatrix} V_S \\ V_E \end{bmatrix} \tag{1}$$

$$I_S = \left(Y_{S,S} - Y_{S,E}Y_{E,E}^{-1}Y_{E,S}\right) V_S + Y_{S,E}Y_{E,E}^{-1}I_E \tag{2}$$

The admittance matrices for the distribution network areas are then reduced in accordance with (2). These boundary buses serve as the interface points to other areas or connections to

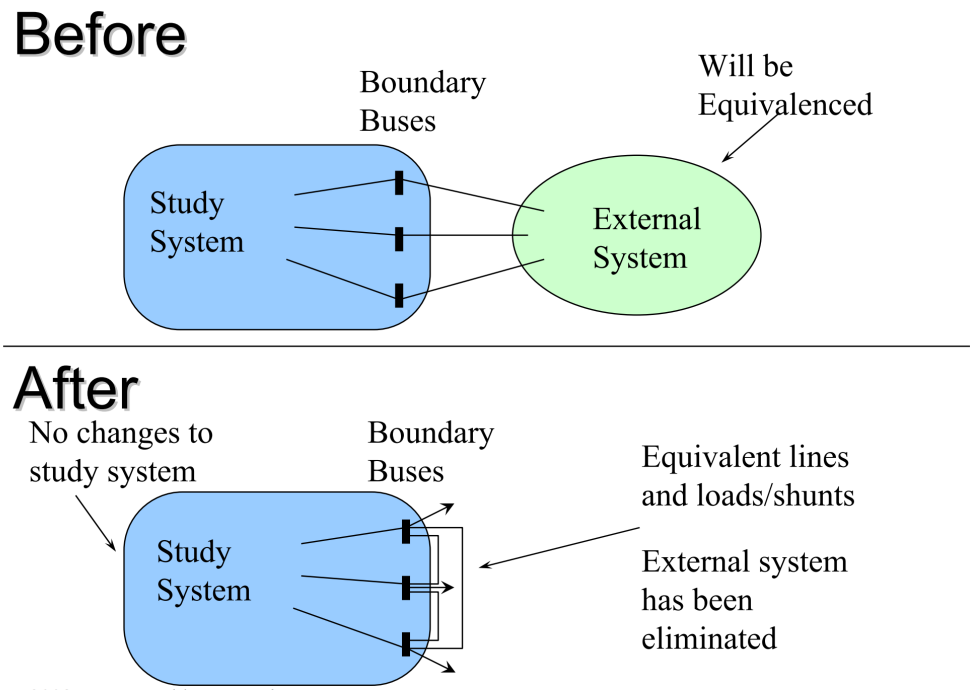

Figure 7: Illustration of the network model reduction process. Image from (PowerWorld Corporation, 2008).

substations. A three-phase area bus is chosen to represent the area load connection, while the remaining area buses and nodes are considered part of the external system.

4.0 Implementation

4.1 Actor Model Environment

To assess the behavior of the distributed approach, we developed a prototype implementation using the Python programming language. This prototype adopts the "actor" model, a mathematical framework for concurrent computation that defines the actor as the fundamental unit of concurrency (Hewitt et al., 1973). Our Python program employs the Pykka implementation (Jodal, 2023) of the actor model, as specified in (dos Reis et al., 2023).

The primary purpose of the actor model environment that we created is to evaluate how the distributed approach performs. This involves determining the time required for the DFLISR use case to restore connectivity to an area during an event and identifying any limitations of the proposed approach. As extensively discussed in (dos Reis et al., 2023), the use case for data configuration and topology identification can provide the actor with information about the system delay, considering the delays resulting from message passing among actors within the same area. This approach ensures that the temporal behavior of the DFLISR use case remains unchanged[2].

Given the specific evaluation objectives, certain simplifications are feasible concerning actor development. Consequently, each area in the system requires only a single area actor for implementing the DFLISR use case. Henceforth, we will refer to the area actor as the "area agent." The area agent is equipped to perform the following tasks:

1. Assess the area's state (i.e., connected or disconnected) and communicate this information to other areas.
    a. Data: Area sensor measurements.
    b. Method: Sensor measurements are time-dependent and influenced by the state of circuit breakers.

2. When disconnected, identify if the area is at fault.
    a. Data: Previous system state and the connection statuses of the system areas.
    b. Method: Network evaluation.

3. When disconnected and not at fault, generate potential reconnection paths and inform other areas.
    a. Data: Current system state and the connection statuses of system areas.
    b. Method: Network evaluation.

4. Evaluate reconnection paths and, upon request from another area, provide the analysis results.
    a. Data: Maximum loads of areas, reduced network models of areas, and paths to evaluate.
    b. Method: Evaluation of reduced-order models.

5. Execute circuit breaker changes if a majority of other areas agree on the reconnection paths.

[2]Although delayed topology information could potentially affect the DFLISR use case's behavior, its effects have been ignored in this report due to the relatively low probability of a fault occurring between the topology change and its recognition by the affected areas.

a. Data: Paths evaluated by a majority of other areas are in agreement.
b. Method: If a feasible agreement exists, circuit breaker(s) are modified.

The network evaluation relies on the NetworkX implementation (Hagberg et al., 2008) in Python. Additionally, the approach includes a communication manager actor responsible for introducing message passing delays and message loss, logging all messages from area agents, and recording the state of the distribution network system (i.e., the states of the circuit breakers).

The approach offers configurable message loss and temporal inputs, which are provided to the actor model environment through JSON input files. These parameters govern temporal message delays and the temporal behavior of the analyses performed by the listed area agent capabilities. This configuration enables the consideration of the time required for executing specific analyses. The configurable inputs encompass the following:

1. Message loss probability
2. Static temporal thresholds
   a. Acceptable time for executing DFLISR changes
   b. Activation of an area evaluation when disconnected to determine if the area is at fault
3. Random uniform distribution
   a. Evaluation of the area state
   b. Generation of potential reconnection paths
   c. Evaluation of reconnection paths
   d. Execution of circuit breaker changes.

The results obtained will elucidate the implications of these temporal parameters and the behavior of the proposed DFLISR use-case actor implementation. It is important to note that the actors are assumed to not behave maliciously.

4.2 Test System

To evaluate the effectiveness of our proposed approach, we conducted a precision assessment using a representative distribution network. Specifically, we utilized the publicly available Midwest 240-Node test distribution system, which replicates an actual distribution network located in the Midwest region of the United States (Wang, 2019; Bu et al., 2019). The system's configuration is visually represented in Figure 8. This test system comprises 240 primary network nodes and encompasses approximately 23 miles of primary feeder conductors. Moreover, the distribution network incorporates a comprehensive dataset with smart meter measurements at the node level, spanning a full year. The load data utilized in our analysis are derived from minute-resolution load data, and the GridLAB-D (Pacific Northwest National Laboratory (PNNL), 2022) version of the Midwest 240-Node test distribution system is publicly accessible in (dos Reis, 2021). The creation of minute-resolution appliance-level load data from the smart meter measurements is detailed in (dos Reis et al., 2020). The source load data originate from nodal hourly smart meter readings. Notably, the minute-resolution load dataset demonstrates a mean absolute percentage error of 2.58% when compared to the nodal hourly smart meter data. The topology of the Midwest 240-Node test distribution system adheres to a radial configuration and comprises three distinct feeders labeled S, M, and L, indicating their

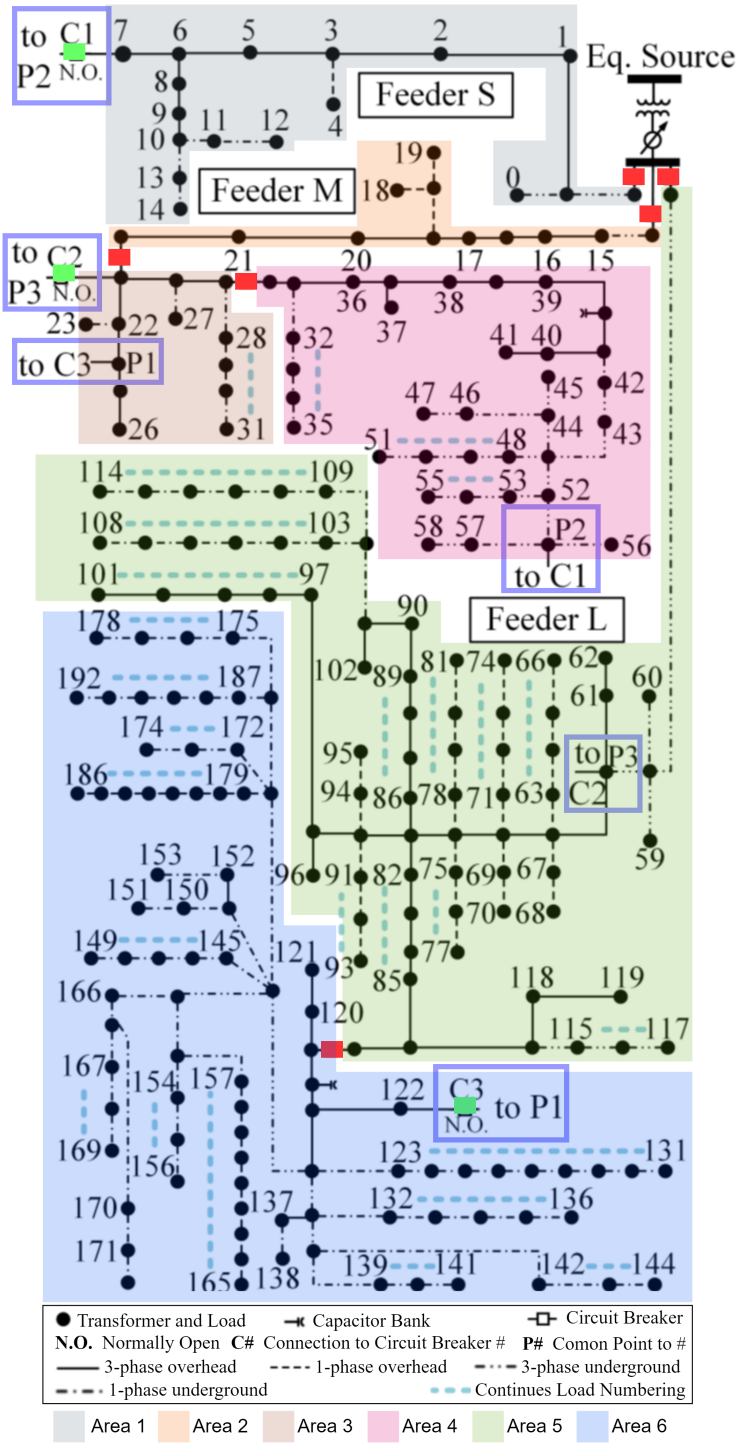

Figure 8: Midwest 240-Node test distribution system. Circuit breakers highlighted in green are normally open, and those highlighted in red are normally closed. Image adapted from (dos Reis et al., 2021).

Table 1: Overview of the Midwest 240-Node test distribution system area.

Feeder	Area	Number of Homes	Area Peak Load	
			kW	kvar
S	1	76	79.41	26.87
M	2	85	36.39	9.63
M	3	23	48.06	15.91
M	4	262	109.61	34.25
L	5	292	281.39	95.75
L	6	382	289.87	95.18

relative sizes (small, medium, and large). For further insights, Table 1 provides an overview of the number of households and peak load values associated with each of these feeder areas.

The Midwest 240-Node test distribution system distinguishes itself from comparable models by virtue of its open accessibility, the availability of load profiles derived from actual smart meter data, and its inclusion of multiple feeders and switch-delimited areas. These attributes make it an ideal choice for assessing the proposed algorithm's effectiveness. Additionally, the system uniquely associates each load bus with the specific households it serves, making it particularly well-suited for evaluating the capacity of DLT-based FLISR to restore customer connections. To address the limitations of the SE algorithm, which does not support split-phase transformers, the loads have been transferred to the primary side of the split-phase transformers.

It is important to highlight that the Midwest 240-Node distribution system exhibits an imbalance, and this extends to the system load as well. The area load imbalance can be calculated using the formula

$$UL = \frac{MD}{AV} \times 100, \tag{3}$$

where UL represents the load imbalance factor as a percentage, MD denotes the maximum deviation of the load, and AV is the average load value. To evaluate the area load imbalance, we considered data from "2017-07-17 16:23:00" to "2017-07-17 17:59:00" at a 1 min resolution. Figure 9 illustrates the load imbalances across different areas during the specified time interval.

4.3 Test System Sensors

The Midwest 240-Node test distribution system is equipped with a comprehensive array of sensors, comprising 51 voltage magnitude sensors (measuring the nodal voltage with respect to a common reference) and 453 active and reactive power sensors. These power monitoring sensors offer insights into the power consumed at or injected into specific nodes, as well as the power flow between nodes. Additionally, circuit breakers are equipped with the capability to measure the voltage magnitude, active power flows, and reactive power flows across their terminals.

Nodal sensors play a pivotal role in recording the active and reactive power levels and are accessible to all nodes within the system, whether they are conventional or virtual sensors. To account for sensor accuracy, a fixed percentage error based on the nominal rating is considered, with an associated uncertainty set at three times the standard deviation. Applying

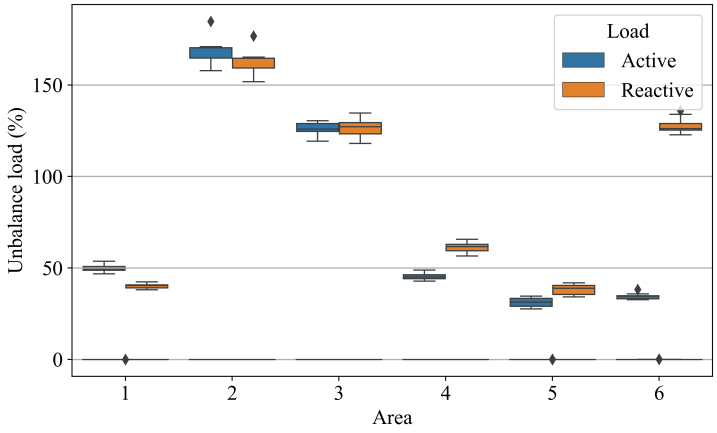

Figure 9: Midwest 240-Node test distribution system. Area evaluation of the active and reactive load unbalances from "2017-07-17 16:23:00" to "2017-07-17 17:59:00" at a 1 min resolution.

this criterion, the empirical rule states that 99.7% of sampled measurements fall within the nominal error rating of the sensors. The per-unit data are summarized in Table 2, utilizing a power base of 63.48 MW.

Voltage sensors are subject to a 1% error with respect to the nominal value, while nodal load values are set at 11 kW, with an expected 5% error relative to the nominal rating. This particular load value is selected to encompass a wide range of nodal load levels, with the absolute maximum nodal load reaching 28.15 kW and the average maximum load node registering at 9.6 kW. The error characteristics for nodal injection/load active and reactive power nodes are uniform, except for nodes connected to capacitors, which exhibit a variance of 17 kvar and a 5% error in the nodal injection/load active and reactive power ratings. The observed maximum power flow at three circuit breaker nodes is 280 kW, with an anticipated 5% error relative to the nominal 280 kW rating. Similar error assumptions are applied to all nodal circuit breaker flows for active and reactive power nodes.

Table 2: Uncertainties associated with the nominal sensor values for the test distribution system.

Sensor Type	Nominal Value (pu)	Percentage Error (%)	Variance
Voltage magnitude	1.0	1	1.11×10^{-5}
Active and reactive power flows for non-capacitor or circuit-breaker nodes	0.00017	5	8.33×10^{-12}
Active and reactive power flows for capacitor nodes	0.00441	5	1.99×10^{-11}
Active and reactive power flows for circuit breaker	0.00026	5	5.4×10^{-9}

5.0 Results

5.1 Comparison of Sequential and Reduced Network Model Area Connection Evaluations

To determine whether an area is suitable for reconnection, we assume that nodal loads are equivalent to the maximum recorded load. However, we set the load equal to the current system load to validate and compare the reduced network model approach with the sequential approach. We use a 1 min resolution and analyze the same period from "2017-07-17 16:23:00" to "2017-07-17 17:59:00" under normal operating conditions and with the circuit breaker states shown in Figure 8. For the sequential approach, the voltage magnitudes for all system nodes are evaluated. Given that the reduced network model approach does not generate voltages to all nodes, the evaluation is performed for the maximum difference node available in the respective area.

The sequential approach utilizing SE is compared to the power flow simulation in the distribution system simulator OpenDSS (Electric Power Research Institute (EPRI), 2022). Figure 10 presents the evaluated absolute voltage magnitude difference between the sequential approach and the outputs from OpenDSS. We observe a maximum absolute difference of 0.000097 pu, which corresponds to a difference of less than 0.01% of the voltage magnitude for all areas of the system. The average difference for all areas is less than 0.0004%. The negligible difference confirms the accuracy and validity of our approach. Given the numerical process used by both the power flow simulation in OpenDSS and SE, such differences were expected. The reduced network model approach utilizing SE is also compared to the outputs from OpenDSS. Figure 11 presents the evaluated maximum difference in the voltage magnitudes of the reduced network model approach and the outputs from OpenDSS. We observe a maximum absolute difference of 0.004268 pu, which is a significant increase in comparison with the sequential approach. The increased difference is expected, given the significant network reduction and the unbalanced characteristics of the test case and its load. The characteristics of the network reduction are presented in Section 3.2.2, and the test case is presented in Section 4.2. The difference is considered acceptable for the purpose of DFLISR, given that an area can be connected if the nodal voltages are within normal operation.

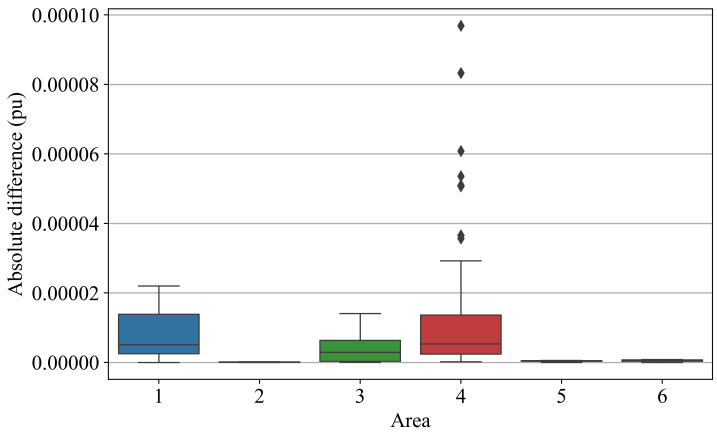

Figure 10: Evaluation of the area voltage difference for the sequential approach. Analyses are from "2017-07-17 16:23:00" to "2017-07-17 17:59:00" with a 1 min resolution.

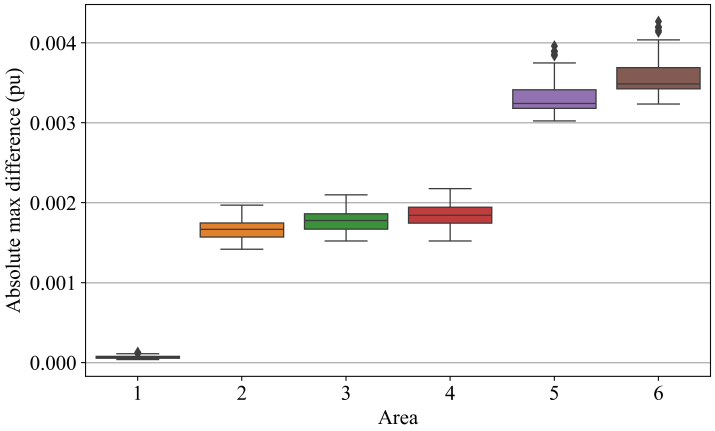

Figure 11: Evaluation of the maximum area voltage difference for the reduced network model. Analyses are from "2017-07-17 16:23:00" to "2017-07-17 17:59:00" with a 1 min resolution.

5.2 Evaluation of the DFLISR Actor Environment

In this section, we present the behavior of area agents across various simulation cases. The results of DFLISR use cases are divided into three components: input configuration variables (specified in JSON file inputs, as described in Section 4.1), message exchanges among agents over time, and the evolution of the test case's state.

The input configuration variables are displayed using a tabular format. The communication between area agents is visualized using an image format, where area agent names are positioned at the top, and the message timestamps are indicated along the y-axis. Message exchanges are represented by arrows; blue arrows denote successfully delivered messages between agents, while red arrows signify lost messages. The arrows connect colored circles, each denoting the type of message being conveyed, categorized into three possibilities: area connection status, request path evaluation, and return of evaluated paths.

The state of the test case is presented as a stacked plot, illustrating the nodal voltages of the test system, with colors distinguishing the represented areas. The topmost plot corresponds to the initial state of the system, featuring time information on the right y-axis. Subsequent plots depict the chronological sequence of system state changes. The bottommost plot illustrates the final state of the system after the completion of DFLISR.

For the evaluated simulation cases discussed below, we commence with the Midwest 240-Node test distribution system in a normal operating condition. Unless otherwise specified for a particular case, the input configuration variables adhere to the settings presented in Table 3. Notably, a permanent fault event occurred in Area 5 at a timestamp corresponding to "2017-07-17 17:00:01," resulting in the disconnection of both Area 5 and Area 6.

Table 3: Default input configuration variables.

Random uniform selection	Range (s)
Evaluate area state	30–60
Generate possible reconnection paths	5–30
Evaluate reconnection paths	10–50
Perform circuit breaker change	5–10
Message passing delay	0.013–2

Static temporal thresholds	Time (min)
Acceptable time to execute DFLISR changes	10
Enable area evaluation when disconnected to identify if the area is at fault	1.5

Message loss	Probability (%)
Between area agents	0.001

Table 4 presents the different parameters used for each of the cases. The intent of the presented simulation cases is to: (1) demonstrate the temporal behavior of the proposed approach, and (2) explore the limitations of the DFLISR.

Table 4: Changes from the default case comparison.

Case	Random uniform selection	Range (s)
1	Message passing delay	0.013–2
2	Message passing delay	5–15
3	Message passing delay	30–60
4	Message passing delay	0.013–2
4	Message passing delay between agents in Areas 1, 2, 3, and 6]	30–60

Case	Message loss	Probability (%)
1	Between area agents	0.001
2	Between area agents	10
3	Between area agents	50
4	Between area agents	0.001
4	Between agents in Areas 1, 2, 3, and 6]	50

5.2.1 Simulation Case 1

In Simulation Case 1, we employ the temporal parameters outlined in Table 3 without any modifications. Figure 12 illustrates the message exchange dynamics among the area agents during this simulation. Following the occurrence of the fault event at "2017-07-17 17:00:01," it takes Area 5 and Area 6 approximately 30–60 s to detect the fault and communicate their state changes to the other area agents. Once the areas self-identify as disconnected, they wait for the defined temporal thresholds to enable self-evaluation. During this phase, they determine whether the area itself is at fault.

Area 5 correctly identifies itself as being at fault and awaits maintenance personnel for the restoration of the connection. In contrast, Area 6 identifies itself as only disconnected. Area 6 proceeds to generate potential reconnection paths and requests other areas to evaluate them. After the evaluation process, the areas return their path assessments to Area 6. Subsequently, Area 6 initiates a circuit breaker state change once a consensus is reached among most other areas, indicating the feasibility of a reconfiguration. Figure 13 visualizes the system's state changes throughout the event. Notably, Area 6 successfully reconnects at "2017-07-17 17:03:33." It promptly self-identifies as reconnected and disseminates this information to the other areas around "2017-07-17 17:04:00." Consequently, the DFLISR use case functions as expected, restoring the connection to Area 6 within a span of 3 min and 32 s.

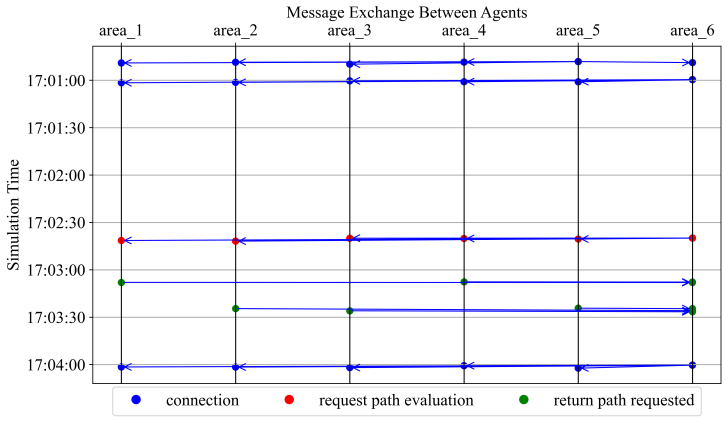

Figure 12: Messages between area agents for Simulation Case 1.

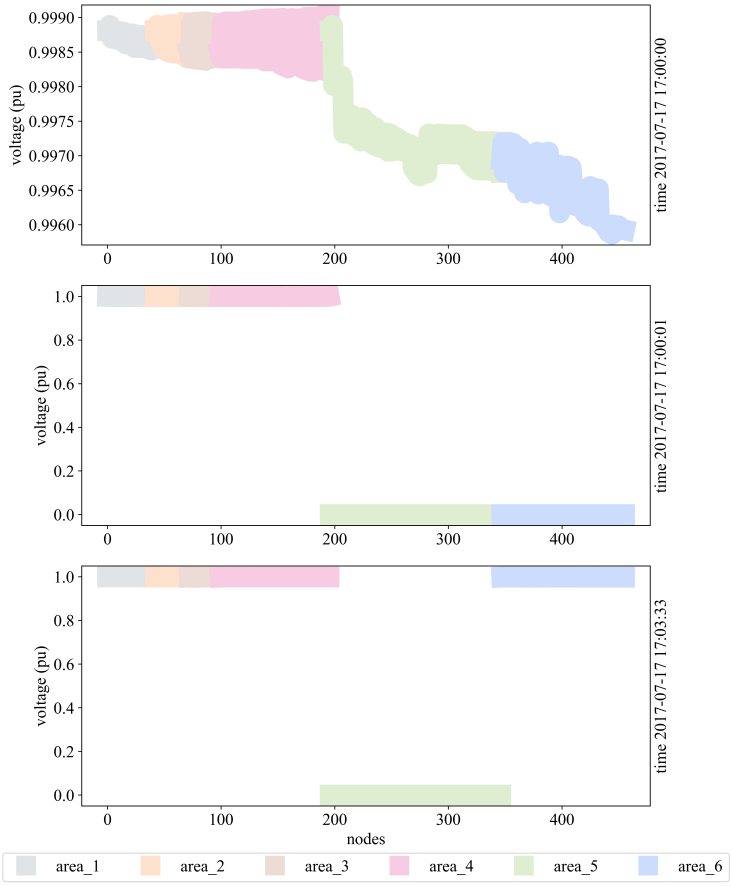

Figure 13: State of the test case for Simulation Case 1. Please note that Area 5 is under fault and thus remains isolated.

5.2.2 Simulation Case 2

Simulation Case 2 involves modifications to the temporal parameters outlined in Table 3, as detailed in Table 5. Specifically, we increased the message passing delay from a range of 0.013–2 s to a range of 5–15 s, and the message loss rate has been elevated from 0.001% to 10%. Figure 14 provides an overview of the message exchange dynamics among the area agents during this simulation. Following the fault occurrence at "2017-07-17 17:00:01," it takes Area 5 and Area 6 approximately 30–60 s to detect the fault and communicate their state changes to the other area agents. However, Figure 14 reveals increased message losses and communication delays as a result of the altered parameters.

Once the areas self-identify as disconnected, they await the defined temporal thresholds to enable self-evaluation, aiming to determine if the area itself is at fault. In this simulation, Area 5 correctly identifies itself as being at fault and patiently waits for maintenance personnel to restore the connection. In contrast, Area 6 recognizes itself as only disconnected. Area 6 proceeds to generate potential reconnection paths and solicits evaluation from the other areas. After evaluation, the areas return their path assessments to Area 6. Subsequently, Area 6 initiates a circuit breaker state change once a consensus is reached among most other areas, signifying the feasibility of a reconfiguration. Figure 15 illustrates the changes in the system's state throughout the event. Notably, Area 6 successfully reconnects at "2017-07-17 17:03:39."

It promptly self-identifies as reconnected and communicates this status to the other areas around “2017-07-17 17:04:15.” Consequently, the DFLISR use case performs as expected, restoring connection to Area 6 within a duration of 3 min and 38 s. Notably, this reconnection occurs 6 s slower than in that Simulation Case 1.

Table 5: Changes in the default input configuration variables for Case 2.

Random uniform selection	Range (s)
Message passing delay	5–15

Message loss	Probability (%)
Between area agents	10

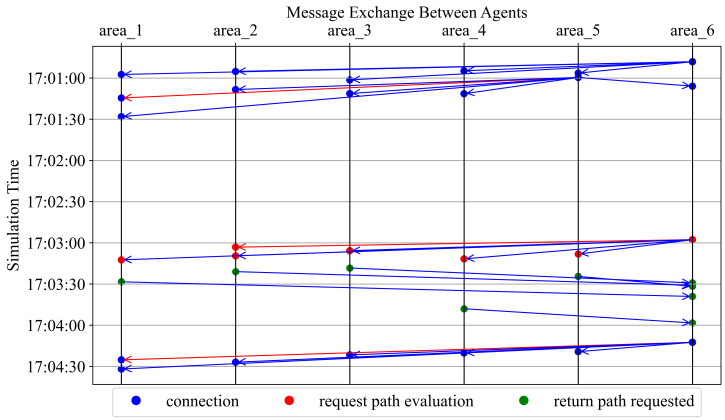

Figure 14: Messages between area agents for Simulation Case 2.

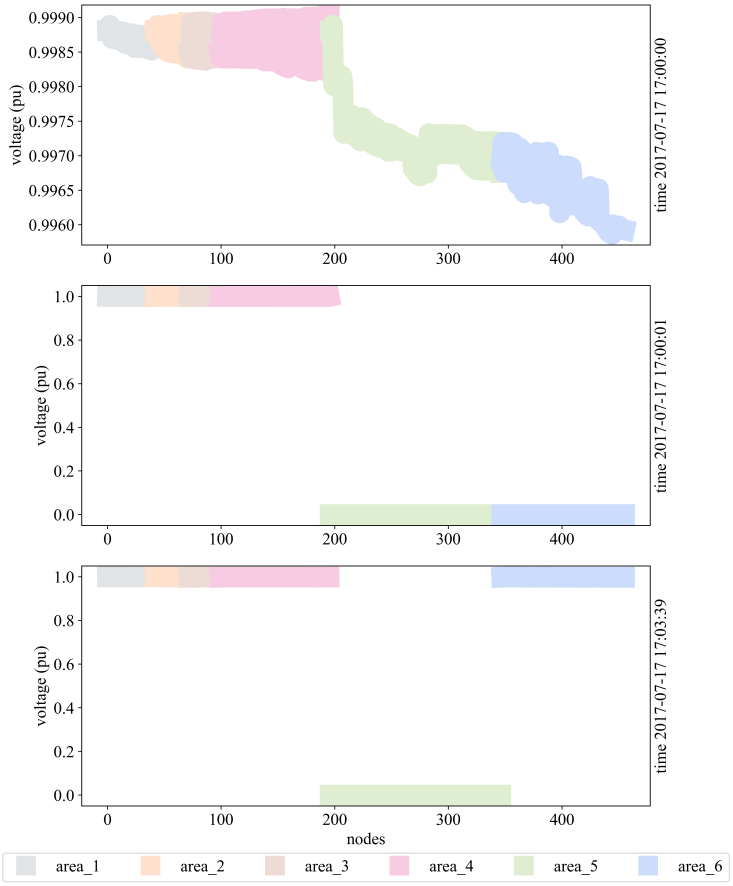

Figure 15: State of the test case for Simulation Case 2. Please note that Area 5 is under fault and thus remains isolated.

5.2.3 Simulation Case 3

Simulation Case 3 introduces significant alterations to the temporal parameters outlined in Table 3. The changes, specified in Table 6, include a substantial increase in the message passing delay, from a range of 0.013–2 s to a range of 30-60 s. Additionally, the message loss rate has been elevated from 0.001% to 50%. Figure 16 provides a detailed depiction of the message exchange dynamics among the area agents during this simulation. Following the fault occurrence at "2017-07-17 17:00:01," Area 5 and Area 6 require approximately 30–60 s to detect the fault and communicate their state changes to the other area agents. The simulation in Figure 16 highlights the substantial increase in message losses, further exacerbating communication delays.

Once the areas self-identify as disconnected, they patiently await the defined temporal thresholds that allow for self-evaluation to determine if the area itself is at fault. In this simulation, Area 5 correctly identifies itself as being at fault and awaits maintenance personnel to restore the connection. However, Area 6 erroneously self-identifies as being at fault. This erroneous identification is attributed to the lack of timely information when Area 6 performs its self-evaluation. Area 6's self-analysis occurs under the assumption of being the only disconnected area, leading to the erroneous identification of a fault. It is important to note that Area 6 becomes aware of Area 5's disconnection significantly later, specifically at "2017-07-17

17:03:30," which is well after the critical timeframe for making an accurate self-assessment. This behavior aligns with the expected outcomes of this simulation case, as the introduced time threshold is essential for preventing areas at fault from erroneously identifying as merely disconnected.

Table 6: Changes in the default input configuration variables for Case 3.

Random uniform selection	Range (s)
Message passing delay	30–60

Message loss	Probability (%)
Between area agents	50

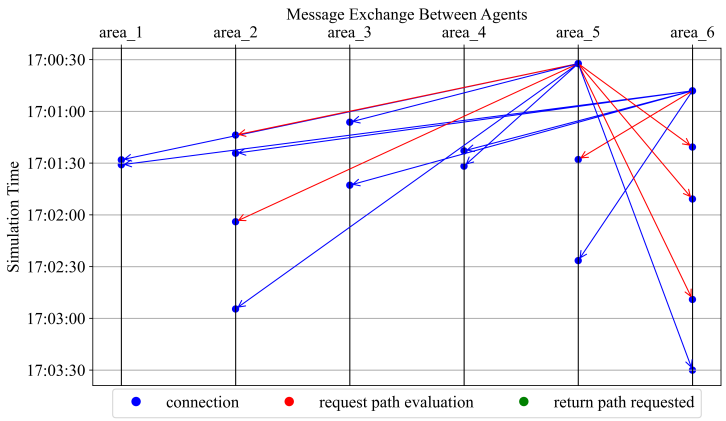

Figure 16: Messages between area agents for Simulation Case 3.

5.2.4 Simulation Case 4

In Simulation Case 4, we introduce significant modifications to the temporal parameters, as specified in Table 7, while initially relying on the parameterization outlined in Table 3. The alterations primarily target the message passing delay and message loss rates between agents in Areas 1, 2, 3, and 6. Specifically, we increase the message passing delay from a range of 0.013–2 s to a range of 30–60 s. Additionally, we elevate the message loss rate from 0.001% to 50%.

Figure 17 provides a detailed visualization of the message exchange dynamics among the area agents during this simulation. Following the fault occurrence at "2017-07-17 17:00:01," both Area 5 and Area 6 require approximately 30–60 s to detect the fault and communicate their state changes to the other area agents. Notably, the increased message loss rate in Figure 17 further exacerbates communication delays, particularly affecting agents in Areas 1, 2, 3, and 6 (i.e., as expected given the Case 4 configuration).

Once the areas self-identify as disconnected, they await the predefined temporal thresholds that enable area self-evaluation. This self-evaluation determines if the area itself is at fault. In this simulation, Area 5 correctly identifies itself as being at fault and awaits maintenance personnel to restore the connection. However, Area 6 accurately self-identifies as only being disconnected. Area 6 subsequently generates possible reconnection paths and solicits the evaluation of these paths from the other areas. After evaluating the paths, the other areas return their path assessments. Area 6 then proceeds to execute circuit breaker state changes once a consensus is reached among most of the other areas, indicating the feasibility of a possible reconfiguration.

Figure 18 illustrates the system's change of state during the event, highlighting the reconnection of Area 6 at "2017-07-17 17:06:20." It's worth noting that the path evaluations from Area 2 and Area 3 arrive after Area 6 has already initiated the circuit breaker changes. Subsequently, Area 6 self-identifies as reconnected and notifies the other areas around "2017-07-17 17:07:15." Consequently, the DFLISR use case in this simulation aligns with expected behavior, successfully restoring connection to Area 6 within a timeframe of 6 min and 19 s. Notably, this reconnection period is 2 min and 42 s longer than that observed in Simulation Case 1.

Table 7: Changes in the default input configuration variables for Case 4.

Random uniform selection	Range (s)
Message passing delay	0.013–2
Message passing delay between agents in Areas 1, 2, 3, and 6]	30–60

Message loss	Probability (%)
Default between area agents	0.001
Between agents in Areas 1, 2, 3, and 6]	50

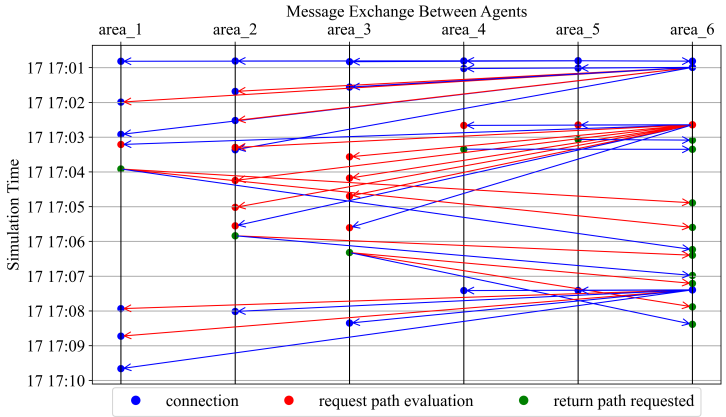

Figure 17: Messages between area agents for Simulation Case 4.

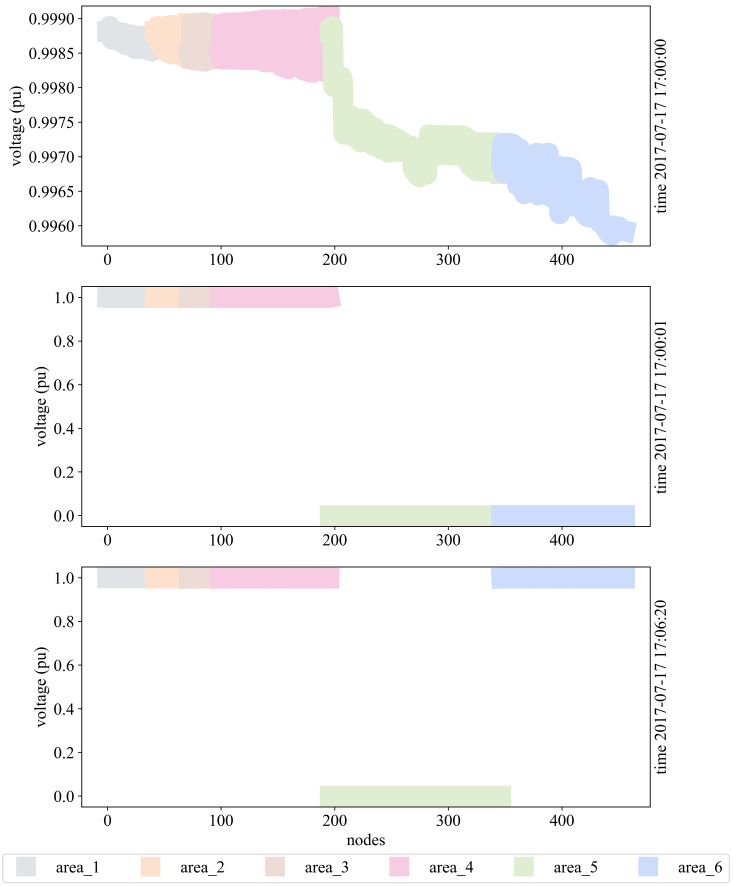

Figure 18: State of the test case for Simulation Case 4. Please note that Area 5 is under fault and thus remains isolated.

6.0 Conclusion and Future Work

This report investigates the potential of DLT as a transformative tool for enhancing fault-tolerant operations in electrical distribution systems. DLT's core attributes, including an immutable and decentralized ledger, distributed consensus mechanisms, and state replication capabilities, have been harnessed to bolster three critical use cases.

A pivotal aspect of our work revolves around the reliance on a consensus-driven ledger, granting actors within the system, such as distributed resources, access to a trustworthy data repository. This enables these actors to collaborate effectively and reach informed decisions by recording outcomes on the blockchain. The first use case focuses on data configuration and employs mathematical criteria—notably, the chi-squared test for gross error detection—to identify sensors with the requisite trustworthiness for advanced decision-making processes. Building upon this foundation of trust, the second use case, topology identification, accurately determines the states of circuit breakers, effectively unveiling the distribution network's topology. Ultimately, the third use case harnesses this established trust to execute switching actions, smoothly reconfiguring feeders and restoring power to disconnected customers following fault events.

The concept of trust is essential in our approach and represents a notable departure from traditional FLISR methodologies. Additionally, the blockchain-based architecture introduces decentralization, empowering disconnected areas to make autonomous decisions, even in scenarios where communication with a central control center is compromised. The primary contributions of this report are (1) a novel approach for evaluating distribution system voltage areas while preserving data ownership and (2) the implementation of interactions between distribution network areas using the actor model. The previous approach for evaluating area connection voltages needed a sequential approach that mandated a radial network topology, limiting its applicability to various distribution system networks. The sequential approach also suffered from increased waiting times for data from preceding areas in the connection path and susceptibility to multiple points of failure if any area along the path failed to provide the necessary analyses. The development of interactions between distributed elements as actors represents a focal point of this study. The developed actor model environment is intended for area-level interactions for the DFLISR use case. Notably, the presented evaluation of the reduced network model area connections resulted in a significant increase in the difference in voltage magnitudes.

The simulation and evaluation of area agents across four distinct simulation cases have provided insights into the area-level interaction behavior during an FILSR event. Simulation Cases 1, 2, and 4 showcase the efficacy of the proposed DFLSR approach in restoring service to Area 6, translating into power restoration for approximately 382 homes. In each simulation case, variations in the message delays and message loss probability are explored, highlighting the impact of slower restoration times. Restoration times in DFLSR scenarios range from 3 min and 32 s to 6 min and 19 s. However, Simulation Case 3 fails to restore Area 6, as the area identifies itself as being at fault, underscoring the challenges associated with area agents performing analyses before obtaining requisite information.

To advance our research and enhance the capabilities of our system, several critical future steps have been identified. One key area of focus involves the development of a robust strategy for reducing the order of the distribution system model, aimed at minimizing disparities between the reduced model and the actual system. This reduction strategy will enable the utilization of the reduced system model in areas demanding higher precision, such as network voltage control and the feasibility of transactive market clearing. The distributed agent representation will be improved by implementing multiple agents per area, fostering consensus-based decision-making within each region. This will be complemented by the

integration of validated sensors into our ledger, providing a reliable data source for decision processes. Continuous updates to sensor behavior and the statuses of switching devices within the ledger will be essential for maintaining situational awareness of the system, enabling the evaluation of the use cases of DLT for both data configuration and topology identification. We aspire to transition from standalone simulations to a co-simulation environment such as GridAPPS-D for a more dynamic and realistic evaluation of system performance.

7.0 References

Abdella, J., Z. Tari, A. Anwar, A. Mahmood, and F. Han (2021). An architecture and performance evaluation of blockchain-based peer-to-peer energy trading. *IEEE Transactions on Smart Grid 12*(4), 3364–3378.

Bhattarai, B., D. J. Sebastian Cardenas, F. B. dos Reis, M. Mukherjee, and S. Gourisetti (2021, December). Blockchain for fault-tolerant grid operations. Report PNNL-32289, PNNL.

Bompard, E., T. Huang, Y. Wu, and M. Cremenescu (2013). Classification and trend analysis of threats origins to the security of power systems. *International Journal of Electrical Power & Energy Systems 50*, 50–64.

Bretas, A. S., N. G. Bretas, B. Carvalho, E. Baeyens, and P. P. Khargonekar (2017). Smart grids cyber-physical security as a malicious data attack: An innovation approach. *Electric Power Systems Research 149*, 210–219.

Bu, F., Y. Yuan, Z. Wang, K. Dehghanpour, and A. Kimber (2019). A time-series distribution test system based on real utility data. In *2019 North American Power Symposium (NAPS)*, pp. 1–6.

Department of Energy (DOE) (2014, November 30). Fault location, isolation, and service restoration technologies reduce outage impact and duration. Report, DOE.

Di Silvestre, M. L., P. Gallo, M. G. Ippolito, R. Musca, E. Riva Sanseverino, Q. T. T. Tran, and G. Zizzo (2019). Ancillary services in the energy blockchain for microgrids. *IEEE Transactions on Industry Applications 55*(6), 7310–7319.

dos Reis, F. B. (2021). A Real-World Test Distribution System with Appliance-Level Load Data for Demand Response and Transactive Energy Studies. doi:10.17632/d57wxwgt4w.1.

dos Reis, F. B., M. Borkum, M. Mukherjee, and D. J. Sebastian Cardenas (2023). Distributed ledger technology for fault tolerant distribution grid operations. *IEEE Access 11*, 63288–63305.

dos Reis, F. B., D. J. Sebastian Cardenas, M. I. Borkum, H. M. Reeve, and M. Mukherjee (2023). Blockchain for fault-tolerant grid operations. Technical report, Pacific Northwest National Lab.(PNNL), Richland, WA (United States).

dos Reis, F. B., R. Tonkoski, B. Bhattarai, and T. M. Hansen (2021). A real-world test distribution system with appliance-level load data for demand response and transactive energy studies. *IEEE Access 9*, 149506–149519.

dos Reis, F. B., R. Tonkoski, and T. Hansen (2020, February). Synthetic residential load models for smart city energy management simulations. *IET Smart Grid 3*(3), 342–354.

Electric Power Research Institute (EPRI) (2022). OpenDSS (Distribution System Simulator). Computer program, available online at: https://www.epri.com/pages/sa/opendss, last accessed on 9/16/2023.

Gonen, T. (2015). *Electric Power Distribution Engineering*. Boca Raton, FL: CRC Press.

Hagberg, A. A., D. A. Schult, and P. J. Swart (2008). Exploring network structure, dynamics, and function using networkx. In G. Varoquaux, T. Vaught, and J. Millman (Eds.), *Proceedings of the 7th Python in Science Conference*, Pasadena, CA USA, pp. 11 – 15.

Hahn, G., A. Werth, E. Piesciorovsky, W. Monday, Y. Polsky, A. Lee, and R. Borges Hink (2022, 9). Oak Ridge National Laboratory Pilot Demonstration of an Attestation and Anomaly Detection Framework using Distributed Ledger Technology for the Power Grid Infrastructure. Technical Report ORNL/TM-2022/2527, Oak Ridge National Lab.(ORNL), Oak Ridge, TN (United States).

Hayes, B., S. Thakur, and J. Breslin (2020). Co-simulation of electricity distribution networks and peer to peer energy trading platforms. *International Journal of Electrical Power & Energy Systems 115*, 105419.

Hewitt, C., P. Bishop, and R. Steiger (1973). A universal modular actor formalism for artificial intelligence. In *Proceedings of the 3rd international joint conference on Artificial intelligence*, pp. 235–245.

Jodal, S. M. (2023). S. M. Pykka Documentation. Computer program, documentation available online at: https://pykka.readthedocs.io/en/stable/, last accessed on 9/16/2023.

Leniston, D., D. Ryan, C. Power, P. Hayes, and S. Davy (2022). Implementation of a software defined FLISR solution on an active distribution grid. *Open Research Europe 1*(142), 142.

Liang, G., S. R. Weller, F. Luo, J. Zhao, and Z. Y. Dong (2019). Distributed blockchain-based data protection framework for modern power systems against cyber attacks. *IEEE Transactions on Smart Grid 10*(3), 3162–3173.

Nour, M., J. P. Chaves-Ávila, and A. Sánchez-Miralles (2022). Review of blockchain potential applications in the electricity sector and challenges for large scale adoption. *IEEE Access 10*, 47384–47418.

Pacific Northwest National Laboratory (PNNL) (2022). GridLAB-D. Computer program, available online at: https://www.gridlabd.org/, last accessed on 9/16/2023.

PowerWorld Corporation (2008). Power system equivalents. Online training, available online at: http://www.powerworld.com/files/TrainingI14Equivalents.pdf, last accessed on 9/16/2023.

Sharma, P. K., M.-Y. Chen, and J. H. Park (2018). A software defined fog node based distributed blockchain cloud architecture for IoT. *IEEE Access 6*, 115–124.

Siano, P., G. De Marco, A. Rolán, and V. Loia (2019). A survey and evaluation of the potentials of distributed ledger technology for peer-to-peer transactive energy exchanges in local energy markets. *IEEE Systems Journal 13*(3), 3454–3466.

Tsai, M.-S. and Y.-T. Pan (2011). Application of BDI-based intelligent multi-agent systems for distribution system service restoration planning. *European Transactions on Electrical Power 21*(5), 1783–1801.

Van Cutsem, O., D. Ho Dac, P. Boudou, and M. Kayal (2020). Cooperative energy management of a community of smart-buildings: A blockchain approach. *International Journal of Electrical Power & Energy Systems 117*, 105643.

Wang, Z. (2019). Iowa Distribution Test Systems. Online, available online at: http://wzy.ece.iastate.edu/Testsystem.html, last accessed on 9/16/2023.

Zhuang, P., T. Zamir, and H. Liang (2021). Blockchain for cybersecurity in smart grid: A comprehensive survey. *IEEE Transactions on Industrial Informatics 17*(1), 3–19.

Pacific Northwest National Laboratory

902 Battelle Boulevard
P.O. Box 999
Richland, WA 99354
1-888-375-PNNL (7665)

www.pnnl.gov